



Electrospun polyvinylidene fluoride/polyacrylonitrile composite fibers: fabrication and characterization

Guizhen Ke¹ · Xinya Jin¹ · Haoxuan Hu¹

Received: 27 May 2019 / Accepted: 18 November 2019 / Published online: 4 December 2019
© Iran Polymer and Petrochemical Institute 2019

Abstract

The purpose of this study is to make use of the advantages of both polyvinylidene fluoride (PVDF) and polyacrylonitrile (PAN) to fabricate a flexible electronic device. Polyvinylidene fluoride (PVDF)/polyacrylonitrile (PAN) composite fibrous mats with different blend ratios were fabricated using electrospinning. The effects of PVDF and PAN mass ratio on fiber morphology, chemical structure, thermal stability, and piezoelectric properties of the produced composite fibers were investigated by scanning electron microscopy (SEM), X-ray diffractometry (XRD), Fourier transform infrared spectroscopy (FTIR), thermogravimetry (TG), and piezoelectric tester. The SEM images showed that the PVDF/PAN composite nanofibers were fabricated successfully and fiber diameters increased with the increase of PVDF content. The FTIR and XRD analyses showed that both the α - and β -crystal phases existed in PVDF/PAN composite fibers. The thermal stability of PVDF/PAN fibrous mats was less than that of neat PVDF fibers. The piezoelectric properties of PVDF/PAN fibrous mats were significant and a function of PVDF content. The output voltage of PVDF/PAN fibrous mats increased from 1.2 to 5.0 V as PVDF content increased from 20 to 100%. The piezoelectric voltages of PVDF/PAN composite nanofibers also increased with the increase of impacting force. Tensile and contact angle testing indicated that the PVDF/PAN fibrous mats were more flexible and hydrophilic than neat PVDF membrane. PVDF/PAN nanocomposite fiber mats were observed suitable for potential application in flexible electronic devices.

Keywords PVDF · PAN · Nanocomposites · Electrospinning · Piezoelectricity

Introduction

Polymer piezoelectric material such as polyvinylidene fluoride (PVDF) was discovered in 1970s. Because of the strong polarity of C–F bond in PVDF and the combination of two fluorine atoms with one carbon atom at the same time, a great dipole moment can be formed in PVDF monomer and there are at least five crystalline phases of alpha, beta, gamma, delta, and epsilon in this semi-crystalline PVDF polymer [1, 2]. In general, it is just a non-polar alpha-crystal phase which exists in PVDF, which does not possess piezoelectric properties. By means of drawing or stretching [3, 4], the incorporation of nanoparticles and other polymers [5, 6] and other methods [7], the PVDF with beta-crystal

phase can be obtained, which has good piezoelectric properties. Compared with traditional piezoelectric materials, PVDF has the advantages of wide frequency response, light weight, good flexibility, and impact resistance. At present, various types of PVDF piezoelectric sensors have been developed and used in many fields such as energy converters [8], motion recognition [9], and human health monitoring [10, 11]. However, the preparation process of PVDF piezoelectric films is complex and costly, and the film has high hardness and poor permeability. In contrast, electrospinning has the advantages of simple operation and low cost, and the electrospun fibers have fine diameter, and continuous and complex porous structures. Thus to fabricate soft and light PVDF membranes with good air permeability, electrospinning method is an ideal choice. At the same time, the electrospinning process integrates polarization and tension, which is beneficial to the fabrication of beta-phase PVDF piezoelectric membrane [12, 13]. In addition, considering pure PVDF membranes cannot meet the special application requirements, many efforts have been devoted to improve

✉ Guizhen Ke
guizhen.ke@wtu.edu.cn

¹ State Key Laboratory for Hubei New Textile Materials and Advanced Processing Technology, Wuhan Textile University, Wuhan 430200, China

the performance of the membranes by blending different polymer components [14, 15]. Among them, polyacrylonitrile (PAN) polymer is a good choice for co-electrospinning. PAN has many unique characteristics: low density, thermal stability, high strength, good chemical and microbial resistance, compatibility with DMF and DMSO, and especially good spinnability. These properties have let PAN to play a role in the production of functional electrospun materials based on PAN [16, 17].

The main objective of this work is to present fabrication and characterization of composite nanofibers electrospun from PVDF and PAN system, and provide important basis for the selection of suitable piezoelectric material. The reports on the production of PVDF and PAN blend composite fibers by single-nozzle co-electrospinning and their piezoelectric properties and other characters are presented. The effect of PVDF and PAN mass ratio on the structure of the electrospun composite nanowebs and the resulting piezoelectric properties were studied in detail. The results can provide useful information for the development of flexible piezoelectric sensors.

Experimental

Materials and chemicals

Polyvinylidene fluoride (PVDF, $M_w = 1,000,000$) powder was purchased from Shanghai Sanfuai New Material Co. Inc., China. *N,N*-Dimethylformamide (DMF) was the analytical reagent and was purchased from Shanghai Chemical Reagent Co. Inc., China. Polyacrylonitrile (PAN, $M_w 50,000$) powder was obtained from Shanghai Plastics Co. Ltd. (Shanghai, China).

Fabrication of PVDF/PAN composite nanofibers

Six gram of PVDF and PAN mixed powder (mass ratio of PAN to PVDF: 0:10, 2:8, 5:5, 8:2 and 10:0, respectively) was added to DMF and the mixture was stirred magnetically until the blend was dissolved completely to obtain a 12 wt% solution. Electrospinning set-up consisted of high-voltage power generator, extrusion pump, syringe (20 mL) with stainless steel needle (0.5 mm inner diameter) on the tip, and fiber collector. Electrospinning of the blended solution was performed at an ambient temperature with an applied voltage of 15 kV, pumping rate of 0.8 mL/h, tip-to-collector distance of 15 cm, and collector rotational speed of 80 rpm. The nanofibers were collected on an aluminum foil wrapped on the collector. After spinning for 12 h, the fibrous mats were collected and kept at an ambient condition for further characterization.

Characterization

Scanning electron microscope (Jeol, JSM-6510LV, Japan) was used to observe surface morphology and microstructure of the electrospun fibrous mats with an accelerated voltage of 30 kV. All the samples were sputter-coated with a thin layer of gold under vacuum before the measurement.

The crystalline phase of PVDF, PAN, and PVDF/PAN nanofiber was analyzed using an X-ray diffractometer (XRD, Dmax-RA, Japan). XRD measurement was carried out at 40 kV per 40 mA with Bragg's angle 2θ from 10° to 90° by a step size of 0.02° .

The chemical structure was confirmed further by Fourier transform infrared (FTIR) spectra of PVDF, PAN, and PVDF/PAN fibrous mats using Avtar360 (SENSOR 27X, Bruker, German). FTIR spectrum of all samples was collected from wavenumber 400 to 4000/cm with a resolution of 4/cm within 32 scans.

Thermal decomposition property of PVDF, PAN, and PVDF/PAN fibrous mats was characterized by thermal gravimetric analysis (NETZSCH STA409PC, German). The TG and DTG curves were recorded starting from the ambient temperature to 800°C with a heating rate of $20^\circ\text{C}/\text{min}$. The flowing rate of protective nitrogen was 50 mL/min.

To evaluate the piezoelectric performance of the PVDF/PAN electrospun mats, a self-made free-falling sphere device was used to connect the oscilloscope to form a piezoelectric testing device. The testing device is schematically shown in Fig. 1. The fibrous mats were cut into $1 \times 1\text{ cm}^2$ pieces and connected on both the sides with the oscilloscope electrode wire. The nanocomposite was mechanically impacted by a small steel hammer with adjustable mass. When the small steel ball falls freely from the catheter onto the surface of the sample, the positive and negative poles of the oscilloscope will transmit the electric signal to the oscilloscope for processing and analysis. The initial position of the small ball is 10 cm from the base and the whole reaction process lasts for 7 ms. The measurement was repeated three times for each sample and the average value was obtained.

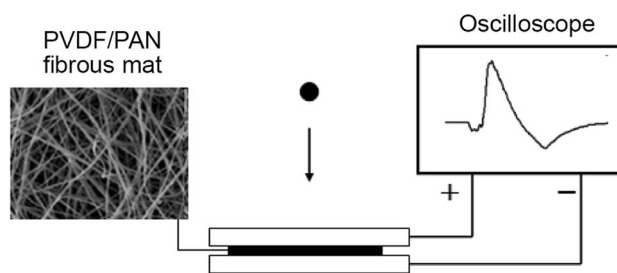


Fig. 1 Schematic representation of the piezoelectric test device

Mechanical properties were determined by a dynamometer (Instron 5566, United States). The tests were performed with a fixed gauge of 20 mm at a loading velocity of 10 mm/min at ambient.

The contact angle of PVDF/PAN composite fiber membrane was measured by a contact angle meter (SL200C, Shanghai Shenrui Instrument Co., Ltd., China) with stationary droplet method. The measurement was repeated three times for each sample and the obtained average values of measurements were reported.

Results and discussion

SEM observation

SEM imaging was used to characterize the nanofiber morphology and structure. The SEM images of electrospun PVDF, PAN, and PVDF/PAN mats are shown in Fig. 2. These images were also analyzed using Image Pro Plus measurement tool to determine the average of fiber diameters. It can be clearly seen that continuous nanofibers were produced and fibers are cylindrical and fine with a relative smooth surface. Several beads can be seen in the webs of the composite fiber with a mass ratio of 8:2 (PAN:PVDF). The density of PVDF/PAN composite fiber with a mass ratio of 5:5 appeared greater, with rougher fiber surfaces compared to the other two composite fiber webs. SEM images were used to obtain the average fiber diameter by analyzing at least 100 fibers using Image Pro Plus. As it can be seen in Fig. 2, the diameters of all fiber samples centered in the nanoscale. Pure PAN (Fig. 2a) has the narrowest fiber diameter distribution and the finest fibers, most of the fiber diameters are in the range of 400–500 nm. As Fig. 2b–d shows, the diameter distribution of PVDF/PAN composite fibers becomes broader and there is an increasing trend in the average values as PVDF content increased. The differences may be caused by the changes of the concentration and viscosity of the blended solution.

XRD analysis

An X-ray diffraction measurement was used to obtain more insight into the structure of the composite nanofibers. The XRD patterns of the composites nanofibers containing different PVDF mass ratio are shown in Fig. 3.

PVDF belongs to polycrystalline polymer and has three different crystalline phases (α , β , and γ). As shown in Fig. 3a, pure PAN has one wide peak at $2\theta=16$, and pure PVDF (Fig. 3e) has three distinct peaks in its spectrum. It is known from the literature that the diffraction peaks of 2θ in the range of 10–45 correspond to the crystal plane from small to large in the order of $\alpha(100)$, $\alpha(020)$, $\alpha(110)$, $\beta(110,200)$,

$\alpha(021)$, $\alpha(130)$, $\alpha(210)$ [18]. Thus the peaks in the pattern of pure PVDF have been centered at $2\theta=14.1$, 16.9, and 20.5 corresponding to reflections of $\alpha(100)$, $\alpha(020)$, and $\beta[(110),(200)]$ PVDF crystalline phases, respectively [19]. This is consistent with the previous report that the beta-crystalline PVDF fibers can be obtained directly from PVDF solution by electrospinning [20]. It is also proved that the electrospinning is a simple and effective method for producing beta-crystalline PVDF fiber membranes. As shown in Fig. 3d, the composite mat with mass ratio of 2:8 (PAN:PVDF) displays strong peaks located at $2\theta=13.9^\circ$ and 16.7° and two weak peaks at 20.0° and 25.6° , implying the dominance of α phase and coexist with a small quantity of β phase. As shown in Fig. 3c, after enlargement, it can be seen that the PVDF/PAN composite mat with mass ratio of 5:5 displays two peaks: one broad peak at $2\theta=17.2^\circ$ and one clear peak at $2\theta=20.4^\circ$, which may be due to the amorphous halo of PAN and β phase of PVDF, respectively. Whereas, the peak for β -crystalline phase is hard to see in Fig. 3b. The composite mat with PAN and PVDF mass ratio 8:2 just shows strong reflections located at $2\theta=14.1^\circ$ and 16.9° and a weak peak at 25.5° , implying the dominance of α phase. The change of PVDF-crystalline phase type in the composite fiber was due to the introduction of PAN, affecting the formation of large-sized crystalline grains in polymer blends.

FTIR study

FTIR is sensitive to the conformation and changes in the molecular region of polymers. Different crystalline phases absorb different infrared wavelengths; thus, FTIR can be used to analyze the structure of crystalline polymers. Typical FTIR spectra of PAN, PVDF/PAN, and PVDF fibrous mats are presented in Fig. 4. Figure 4a shows that the typical peaks of PAN spectrum have been centered at about 2240, 2942, and 1448/cm, corresponding to $-C\equiv N$ bond stretching vibration, $-CH_2$ bond asymmetric and symmetric bending vibrations, respectively. The PAN characteristic peaks have also been displayed in the spectrum of PVDF/PAN fibrous mats (Fig. 4b). The characteristic peaks in PVDF/PAN samples spectra at 1401 and 1178/cm are strengthened, ascribing to the C–H bond bending vibration and C–F bond stretching vibration, respectively. Spectrum results indicated that the PAN and PVDF structures are reserved in the composite fiber, and PAN and PVDF have a good adaptation.

According to the literature [21], the characteristic peaks at 1383, 976, 853, 796, 762, 612, and 530/cm correspond to the α crystal form of PVDF, and those at 1278, 839, 510, and 471/cm correspond to the β crystal form. As shown in Fig. 4c, the peak observed at wavenumber 769/cm is assigned to α phase with chain conformations of short trans-sequences. The peaks appearing at wavenumbers 1275, 836, 509, and 475/cm correspond to the β phase with long

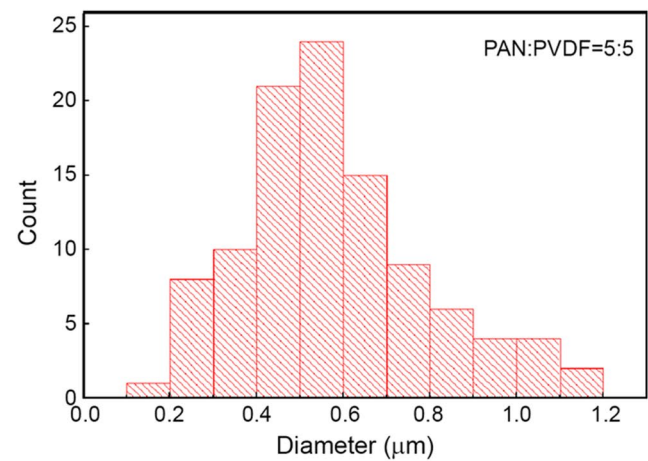
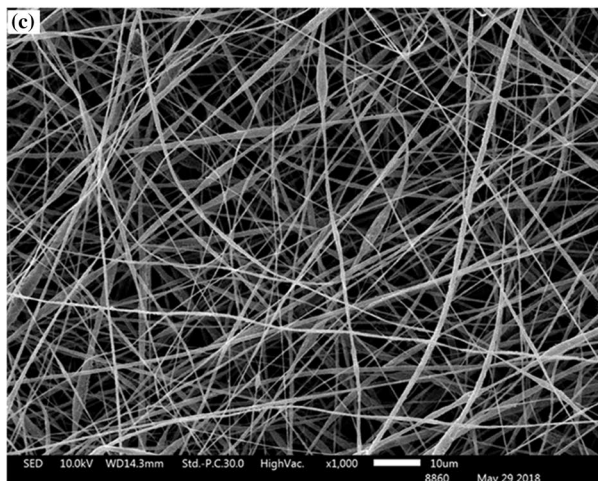
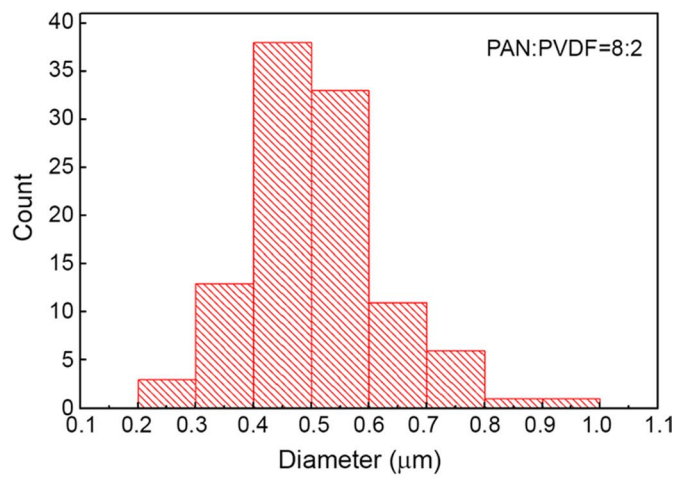
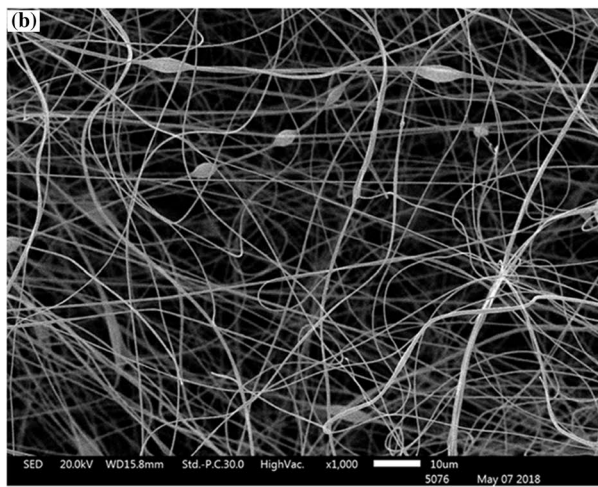
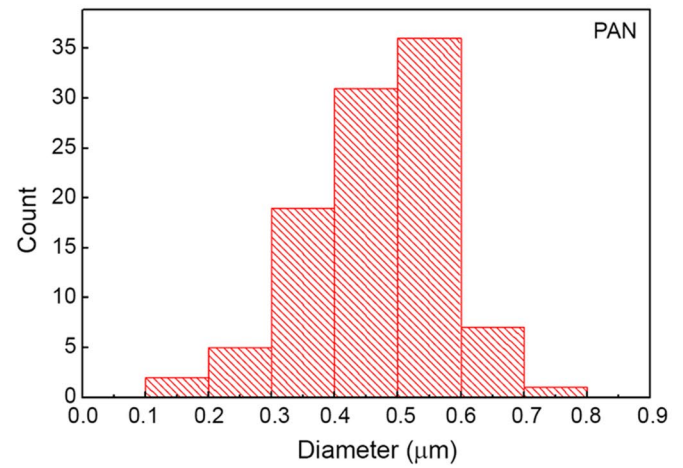
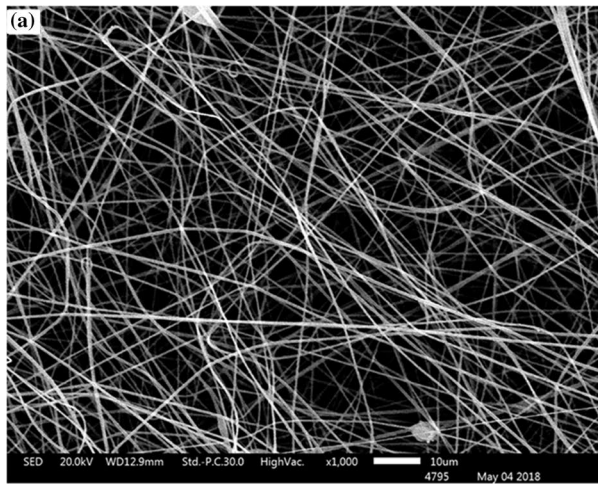


Fig. 2 SEM images of electrospun webs: **a** PAN; **b** PAN:PVDF = 8:2; **c** PAN:PVDF = 5:5; **d** PAN:PVDF = 2:8; **e** PVDF

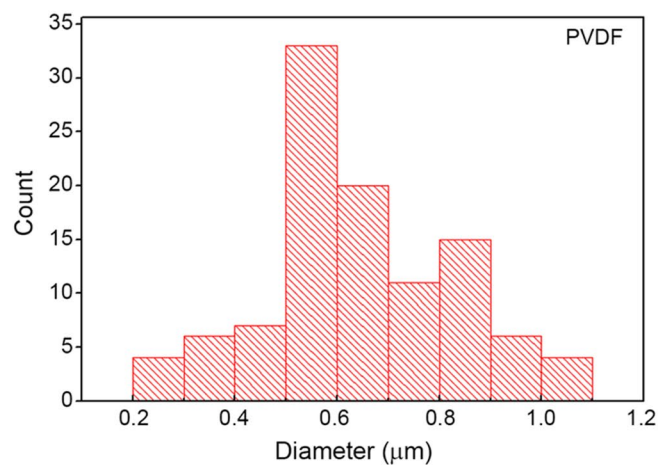
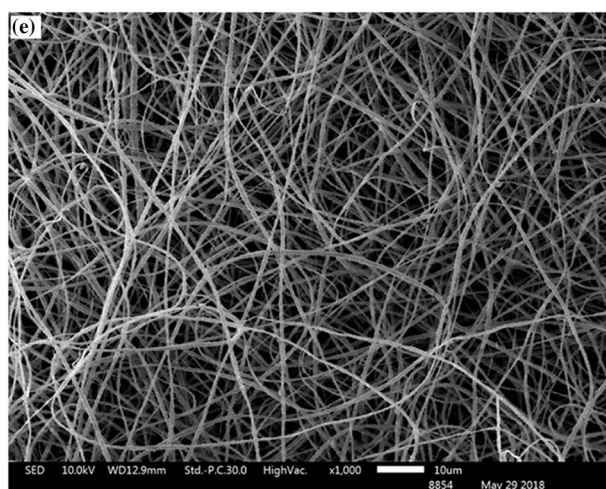
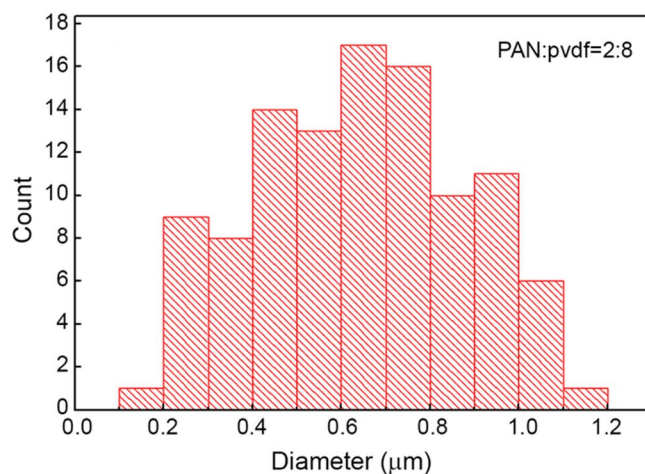
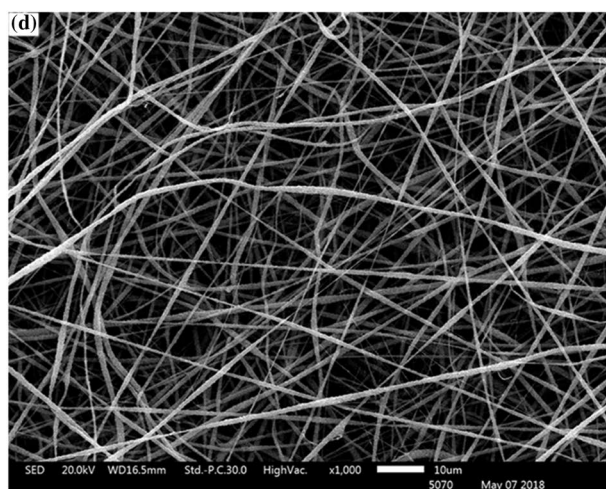


Fig. 2 (continued)

trans-sequences. The FTIR spectra of PVDF/PAN composites (Fig. 4d) exhibited almost the same spectral features as PVDF, regardless of the PAN content. By observation of the relative intensity of the beta peaks, there is an increasing trend with the increase of PVDF content. The results indicate a good consistency between those of the FTIR and X-ray diffraction testing. It is known that the piezoelectric properties come from the β phase of the PVDF. The results from XRD and FTIR measurement indicate that the PVDF/PAN composite mats have potential piezoelectric functions.

Thermal stability

The relationship between mass residues and temperature was measured to investigate the thermal stability of neat PAN, PVDF/PAN nanocomposites and neat PVDF by means of TG and DTG as displayed in Fig. 5. As it

is evident in Fig. 5, there are two main thermal degradation areas with about 50% weight loss for neat PAN and PAN:PVDF = 8:2 composite fibers: the minor one between 280 and 330 °C and the major one between 370 and 460 °C, which was attributed to the volatilization of gaseous compounds during the heating process. For PVDF/PAN composite fiber with mass ratio of 5:5 and 2:8, a major wide mass degradation peak happened between 280 and 460 °C. For neat PVDF, one major sharp mass degradation peak was observed between 410 and 500 °C. The decomposition of all samples was nearly completed at 500 °C. Thermal stability can be judged by the initial decomposition temperature and thermal degradation temperature at 5% mass loss [22]. Considering these two parameters, the composite fiber with higher PVDF content shows better thermal stability than neat PAN nanofiber.

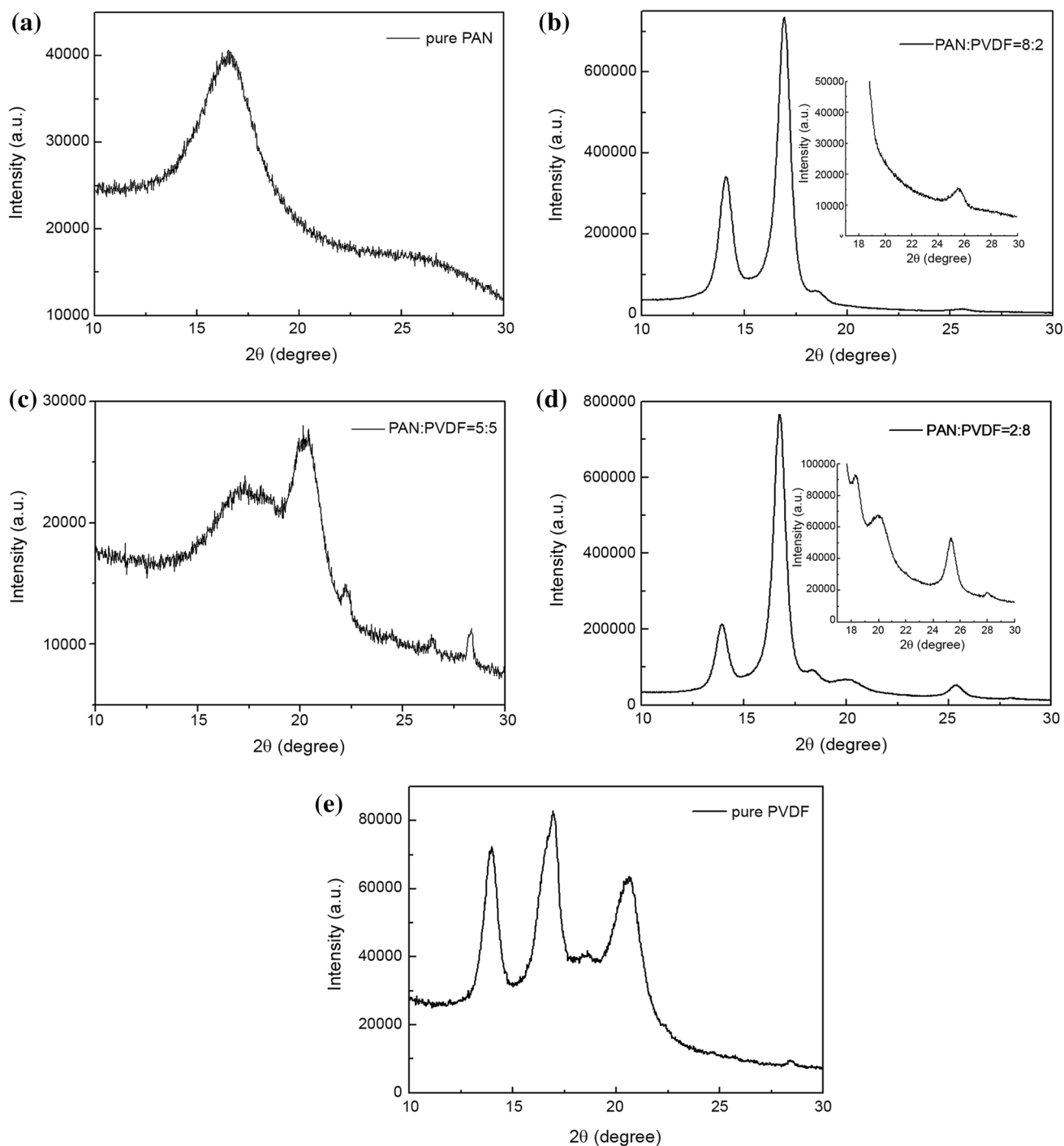


Fig. 3 XRD patterns of electrospun fibrous mats: **a** PAN; **b** PAN:PVDF = 8:2; **c** PAN:PVDF = 5:5; **d** PAN:PVDF = 2:8; **e** PVDF

Mechanical properties

The mechanical properties of the nanofiber mats were measured and the tensile stress–strain curves of the electrospun mats are presented in Fig. 6. It can be seen that the PVDF, PAN, and PVDF/PAN mats show typical thermoplastic behavior. Comparing them with a neat PAN fiber mat, PVDF

and PVDF/PAN composites present stiffening characteristics such as greater elastic modulus and less elongation-at-break. Compared with polyvinylidene fluoride (PVDF), the flexibility of PAN is more prominent. The mechanical properties of the electrospun mats are a result of the complex effect of many parameters such as average fiber diameter value, diameter distribution, porosity, and the degree of polymer

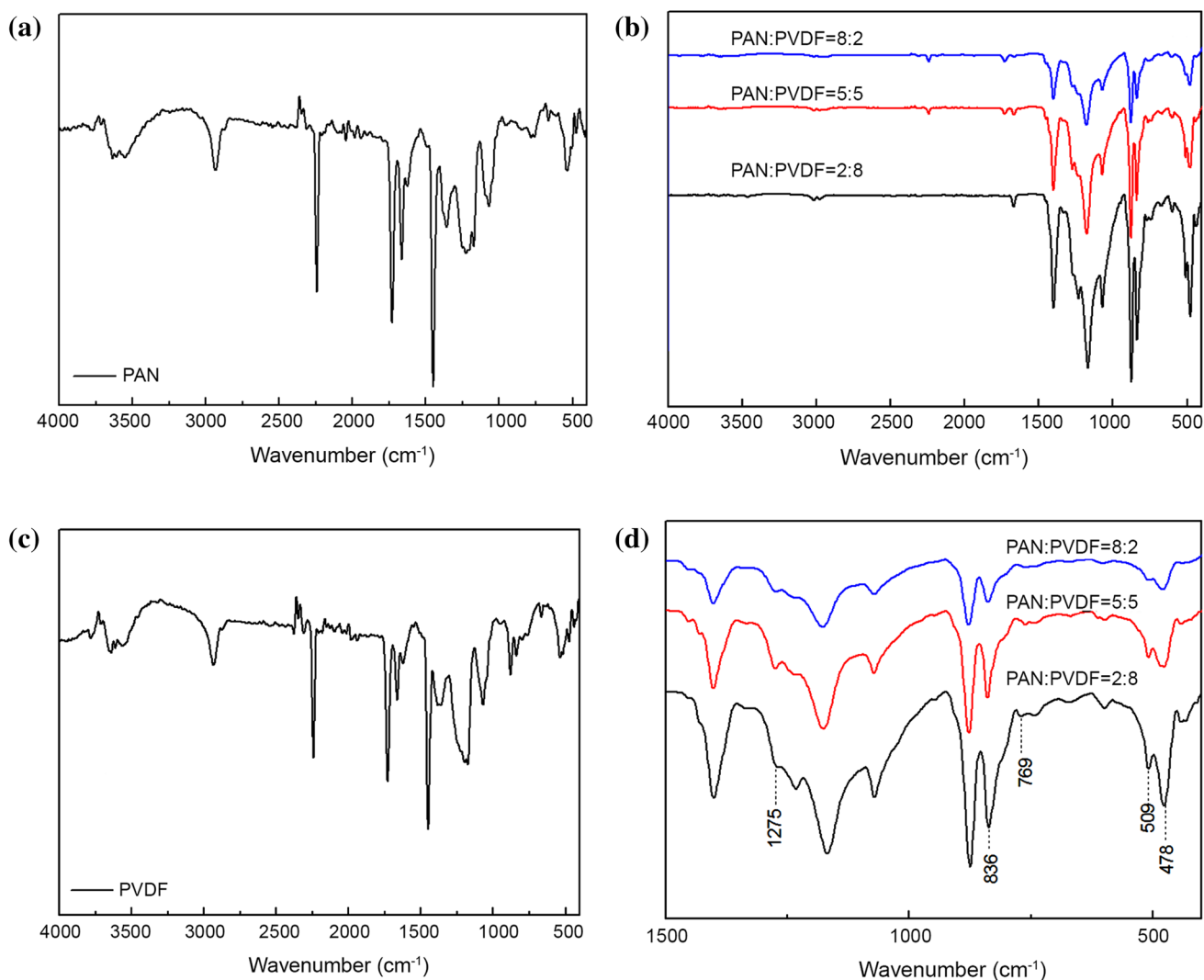


Fig. 4 FTIR spectra of electrospun PVDF/PAN fibers: **a** PAN; **b** PVDF/PAN composite mats; **c** PVDF; **d** enlargement of spectra of PVDF/PAN composite mats

crystallinity, thus PVDF/PAN composite nanowebbs have complex mechanical behavior. Generally, though the addition of PAN may decrease the piezoelectric function, the flexibility of the composite mats can be improved and the obtained composites could be more suitable for applying in polymer electrolytes in self-power devices.

Hydrophilicity

The water contact angles measured for all samples are presented in Fig. 7. Since the molecular chains of PVDF are composed of hydrocarbon bonds and CF bonds, the hydrophilicity of pure PVDF fibrous mat is poor due to the absence of hydrophilic groups. The measured water contact angle is as high as 133. While the cyanogen group with hydrophilicity exists in PAN molecule, with the increase of

PAN content, the contact angle begins to decrease till 116 when the mass ratio of PAN and PVDF reaches 8:2. Therefore, the hydrophilicity of PVDF/PAN nanocomposites can be adjusted by the addition of PAN.

Piezoelectricity

A steel ball of 5.61 g was used to impact the PVDF and PVDF/PAN nanocomposite fibrous mats between two metal electrodes, and the output voltage measured by the oscilloscope is shown in Fig. 8. When the fibrous membrane was impacted by the small steel ball, the elastic deformation caused the change in dipole of the beta crystal of the fiber and produced the piezoelectric effect. The voltage curve corresponds to three states of impacting process: original state, compression state, and rebound

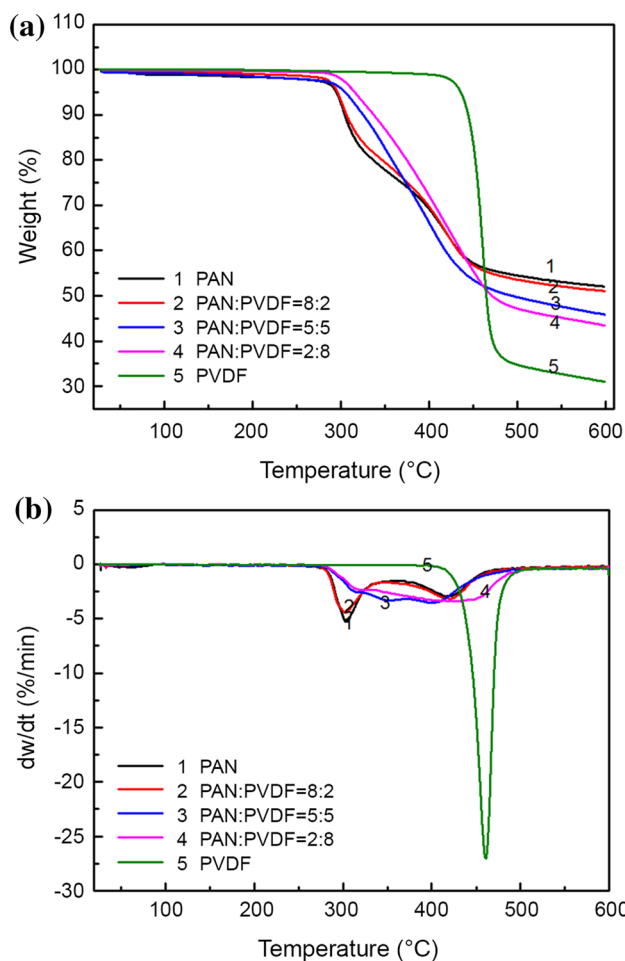


Fig. 5 Thermograms of electrospun PVDF/PAN fibers: **a** thermogravimetric (TG) analysis, **b** derivative thermogravimetric (DTG) curves

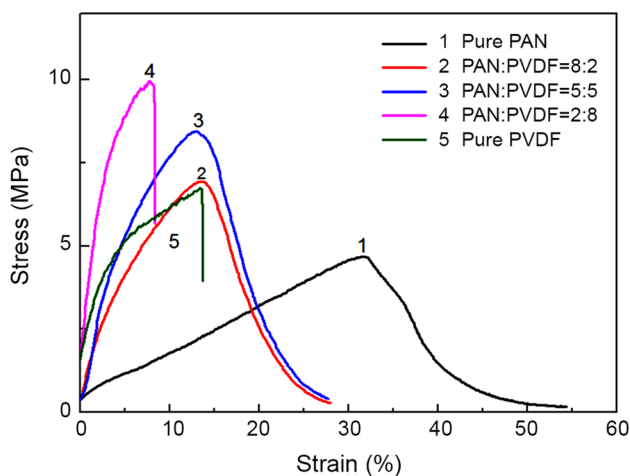


Fig. 6 Mechanical stress–strain curves of electrospun fibrous mats

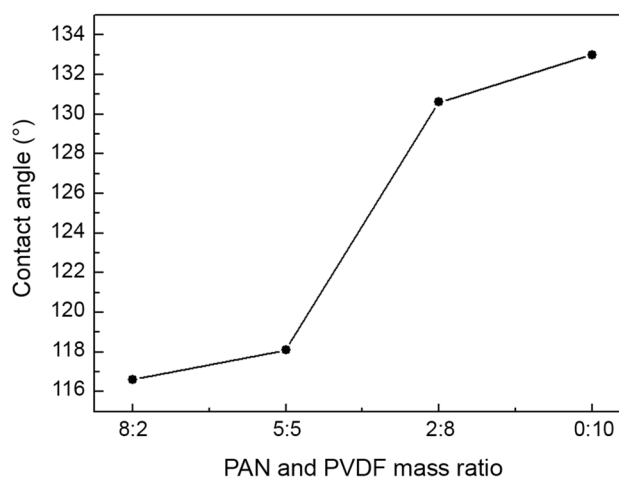


Fig. 7 Contact angle of electrospun PVDF/PAN composites

state. Before the sphere reaches the surface of the fibrous mat, there is no potential difference between the two ends of the fibrous mat and the voltage value is zero. When the sphere contacts the surface of fibrous mat, the fibrous mat is impacted by a small ball and begins to compress downward, resulting in a negative voltage. Since the deformation of the fibrous mat belongs to elastic deformation, when the velocity of the ball decreases to zero, the fibrous mat begins to rebound and the voltage signal turns into a positive voltage. As the deformation rate increases gradually, the positive voltage gradually increases to the maximum value. It is obvious that the output voltage of the generators increases from 1.2 to 5.0 V with the increase of PVDF content in the fibrous mats from 20 to 100%. These outputs can be compared to the voltage output of previous literature [23]. The more efficient electrical outputs can be interpreted by higher β -phase crystallinity in PVDF/PAN composite fiber.

To investigate the effect of impact pressure on the piezoelectricity, the steel ball with different masses was used on the PVDF/PAN composite fiber with a mass ratio of 2:8 (PAN:PVDF). The results are shown in Fig. 9. The increase of ball mass resulted in a greater compression force and rebound force on the nanofibrous mat; therefore, the negative voltage during the compression process and output positive voltage during rebound process increase correspondingly. The piezoelectric response process also becomes longer. When the mass of the small ball is 14 g, the maximum voltage value reaches 9 V. Excellent piezoelectricity can produce micro-current effect, which indicates that the PVDF/PAN composites can be used as a potential electrical generator and to charge portable electronic devices.

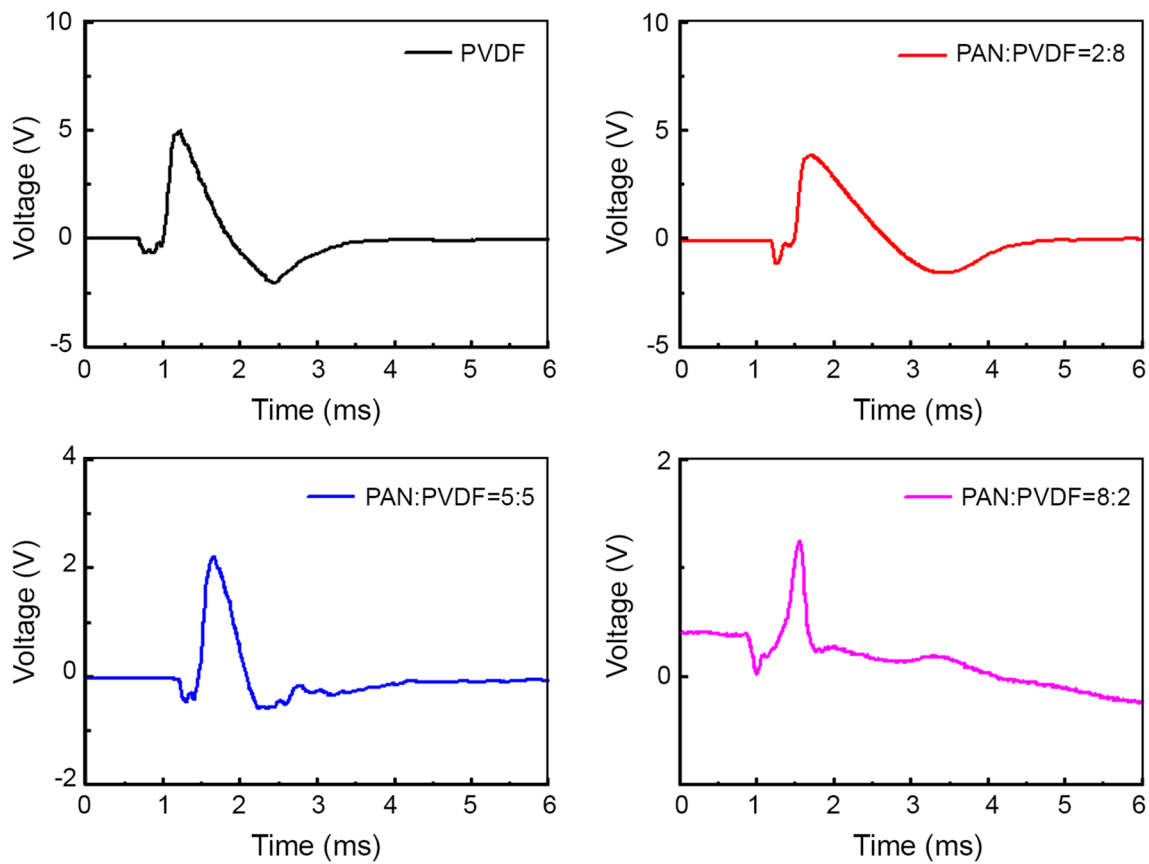


Fig. 8 Piezoelectric voltages of PVDF/PAN fibrous mats

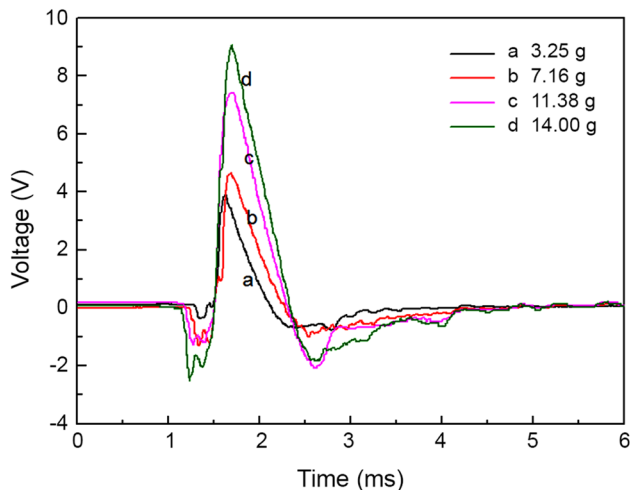


Fig. 9 Effect of small ball mass on piezoelectric voltages

Conclusion

PVDF has displayed an effective approach towards textile flexible sensor. Electrospinning of PVDF and other polymers with good spinnability provides a new method for fabrication of piezoelectric membrane. Based on these, PVDF/PAN nanocomposites were fabricated using electrospinning successfully. Performance characterizations indicated that the addition of PAN reduced the toughness and water repellency of the nanocomposites. The thermal stability of PVDF/PAN fibers was similar to that of neat PAN nanofibers. XRD and FTIR analyses showed that the electrospun PVDF and PVDF/PAN fibrous mats possessed β -phase crystalline structure. Neat PVDF and PVDF/PAN nanocomposites demonstrated good piezoelectricity. The piezoelectric properties of PVDF/PAN nanocomposites could be adjusted through PVDF and PAN mass ratio. The electrical outputs of PVDF/

PAN were related to the impact force. Electrospun PVDF/PAN nanocomposite fiber mats demonstrate a promise for potential application in flexible wearable electronic devices.

Acknowledgements This work was financially supported by Hubei Natural Science Foundation and Fundamental Research Funds of Wuhan Textile Universities. Authors are thankful to Prof. Zikui Bai for providing piezoelectric characterization facility.

References

- Ruan L, Yao X, Chang Y, Zhou L, Qin G, Zhang X (2018) Properties and applications of the β -phase poly(vinylidene fluoride). *Polymers* 10:1–27
- Gregorio R (2006) Determination of the α , β , and γ crystalline phases of poly(vinylidene fluoride) films prepared at different conditions. *Proteomics* 100:3272–3279
- da Silva AB, Wisniewski C, Esteves JVA, Gregorio R (2010) Effect of drawing on the dielectric properties and polarization of pressed solution cast beta-PVDF films. *J Mater Sci* 45:4206–4215
- Du CH, Zhu BK, Xu YY (2007) Effects of stretching on crystalline phase structure and morphology of hard elastic PVDF fibers. *J Appl Polym Sci* 104:2254–2259
- He LH, Qun X, Hua CW, Song R (2010) Effect of multi-walled carbon nanotubes on crystallization, thermal, and mechanical properties of poly(vinylidene fluoride). *Polym Compos* 31:921–927
- Sun J, Yao L, Zhao QL, Huang J, Song R, Ma Z, He LH, Huang W, Hao YM (2011) Modification on crystallization of poly(vinylidene fluoride) (PVDF) by solvent extraction of poly(methyl methacrylate) (PMMA) in PVDF/PMMA blends. *Front Mater Sci* 5:388–400
- Song R, Liu X, Wang HF, Xia GM, He LH, Wang Y, Huang W, Zhao QL (2014) Enhanced beta phase of polyvinylidene fluoride with addition of polyamide 6: role of interfacial interactions. *Colloid Polym Sci* 292:817–828
- Zabek D, Taylor J, Le Boulbar E, Bowen CR (2015) Micropatterning of flexible and free standing polyvinylidene difluoride (PVDF) films for enhanced pyroelectric energy transformation. *Adv Energy Mater* 5:1401891
- Dong WT, Xiao L, Hu W, Zhu C, Huang YA, Yin ZP (2017) Wearable human–machine interface based on PVDF piezoelectric sensor. *T I Meas Control* 39:398–403
- Lopes AC, Gutierrez J, Barandiaran JM (2018) Direct fabrication of a 3D-shape film of polyvinylidene fluoride (PVDF) in the piezoelectric beta-phase for sensor and actuator applications. *Eur Polym J* 99:111–116
- Fu YM, He HX, Zhao TM, Dai YT, Han WX, Ma J, Xing LL, Zhang Y, Xue XY (2018) A self-powered breath analyzer based on PANI/PVDF piezo-gas-sensing arrays for potential diagnostics application. *Nano Micro Lett* 10:1–12
- Motamedi AS, Mirzadeh H, Hajiesmaeilbaigi F, Bagheri-Khoulenjani S, Shokrgozar M (2017) Effect of electrospinning parameters on morphological properties of PVDF nanofibrous scaffolds. *Prog Biomater* 6:113–123
- Gee S, Johnson B, Smith AL (2018) Optimizing electrospinning parameters for piezoelectric PVDF nanofiber membranes. *J Membr Sci* 563:804–812
- Xing J, Ni QQ, Deng BY, Liu QS (2016) Morphology and properties of polyphenylene sulfide (PPS)/polyvinylidene fluoride (PVDF) polymer alloys by melt blending. *Compos Sci Technol* 134:184–190
- Sun D, Yue DM, Li BB, Zheng ZS, Meng XC (2019) Preparation and performance of the novel PVDF ultrafiltration membranes blending with PVA modified SiO₂ hydrophilic nanoparticles. *Polym Eng Sci* 59:E412–E421
- Sidorina AI, Druzhinina TV (2016) Macrostructure of polyacrylonitrile nanofibers produced by electrospinning. *Fibre Chem* 47:362–366
- Choi S, Kim HR, Jeong YK (2018) Mechanism of electrospinning for poly(amic acid)/polyacrylonitrile fiber fabrication. *J Macromol Sci Part B Phys* 57:222–230
- Guo ZW, Nilsson E, Rigdahl M, Hagström B (2013) Melt spinning of PVDF fibers with enhanced β phase structure. *J Appl Polym Sci* 130:2603–2609
- Hossein F, Mohammad MA, Parastoo S, Nima Z, Li QX, Minoo N (2016) Morphological changes towards enhancing piezoelectric properties of PVDF electrical generators using cellulose nanocrystals. *Cellulose* 23:3625–3637
- Neppalli R, Wanjale S, Birajdar M, Causin V (2013) The effect of clay and of electrospinning on the polymorphism, structure and morphology of poly(vinylidene fluoride). *Eur Polym J* 49:90–99
- Layek RK, Samanta S, Chatterjee DP, Nandi AK (2010) Physical and mechanical properties of poly(methyl methacrylate)-functionalized graphene/poly(vinylidene fluoride) nanocomposites Piezoelectric beta polymorph formation. *Polymer* 51:5846–5856
- Gaur MS, Indolia AP, Rogachev AA, Rahachou AV (2015) Influence of SiO₂ nanoparticles on morphological, thermal, and dielectric properties of PVDF. *J Therm Anal Calorim* 122:1403–1416
- Wang G, Liu T, Sun XC, Li P, Xu YS, Hua JG, Yu YH, Li SX, Dai YZ, Song YX, Lv C, Xia H (2018) Flexible pressure sensor based on PVDF nanofiber. *Sens Actuator A Phys* 280:319–325